



Visible-to-UV photon upconversion in metal-free molecular aggregates based on glassy diphenylnaphthalene derivatives

Journal:	<i>Journal of Materials Chemistry C</i>
Manuscript ID	TC-COM-05-2024-001820.R1
Article Type:	Communication
Date Submitted by the Author:	23-Jun-2024
Complete List of Authors:	Watanabe, Shun; Kyushu University Mizukami, Kiichi; Kyushu University Kimizuka, Nobuo; Kyushu University - Ito Campus, Chemistry and Biochemistry Yasuda, Takuma; Kyushu University, Institute for Advanced Study

SCHOLARONE™
Manuscripts

COMMUNICATION

Visible-to-UV photon upconversion in metal-free molecular aggregates based on glassy diphenylnaphthalene derivatives

Shun Watanabe,^a Kiichi Mizukami,^a Nobuo Kimizuka*^a and Takuma Yasuda*^{a,b}Received 00th January 20xx,
Accepted 00th January 20xx

DOI: 10.1039/x0xx00000x

Visible-to-ultraviolet photon upconversion (UC) based on triplet-triplet annihilation was demonstrated in metal-free glassy solid films consisting of an organoboron photosensitizer and diphenylnaphthalene-based emitter. Upon photoexcitation at 445 nm, UC emissions in the ultraviolet region (370–390 nm) were observed in binary solid films with high UC efficiencies of up to 2.6% and a threshold excitation intensity as low as 44 mW cm⁻².

Photon upconversion (UC) is a versatile photophysical process that can convert lower-energy photons into higher-energy photons.¹ Triplet-triplet annihilation upconversion (TTA-UC), also known as triplet fusion UC, has recently attracted significant attention because of its advantages over other UC techniques, including low excitation intensity requirement, high UC quantum yield (Φ_{UC}), and tunable UC emission wavelength.^{2–14} In particular, TTA-UC from visible to ultraviolet (UV) light has been applied to photocatalytic systems.^{15–20} For further expansion of applications, it is desirable to construct efficient solid-state TTA-UC systems that are completely different from those in conventional liquid media (diffusion-dependent systems). To date, various approaches to solid-like (or quasi-solid) TTA-UC have been attempted, including using polymer matrix,^{21–36} gel matrix,^{37–39} and solid film systems.^{40–43} However, few reports exist on efficient solid-state visible-to-UV TTA-UC that can be driven with substantially low excitation power.^{27,43}

Here, we report a simple but efficient all-solid-state visible-to-UV TTA-UC system that does not require an additional host matrix nor a toxic metal-complex photosensitizer (Fig. 1). This novel TTA-UC system features metal-free binary solid mixtures of an organoboron photosensitizer (**BBCz-SB-Br**) doped into an amorphous organic emitter (**SiDPN-1** and **SiDPN-2**). The

photosensitizer absorbs incident light and subsequent intersystem crossing (ISC) forms the triplet (T_1) excitons, which are then transferred to the emitter via triplet energy transfer (TET); TTA between two T_1 excitons produces a higher-energy singlet (S_1) exciton on the emitter, resulting in UC emission (Fig. 1b). Unlike conventional solutions, our TTA-UC system does not require fluidic molecular diffusion and functions in the form of transparent glassy solid films.

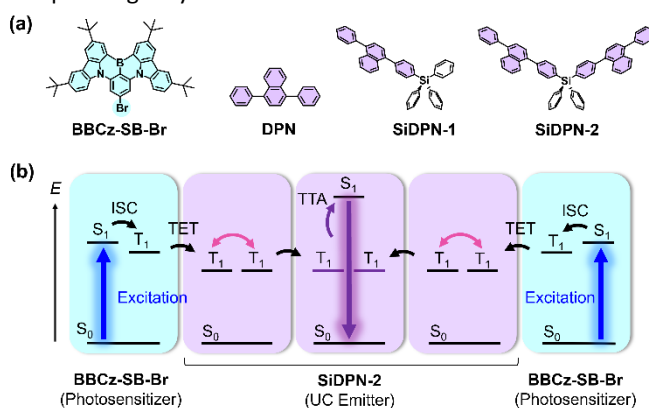


Fig. 1. (a) Molecular structures of a photosensitizer and emitters used in solid-state TTA-UC systems. (b) Mechanistic diagram of TTA-UC in the **BBCz-SB-Br:SiDPN-2** binary system.

BBCz-SB-Br,⁴⁴ which is employed as a photosensitizer in this study, is originally an organoboron-based multi-resonance thermally activated delayed fluorescence (MR-TADF) material,^{45–47} that can populate its T_1 states with $\sim 100\%$ intersystem crossing (ISC) quantum yield because of the small singlet–triplet energy gap (ΔE_{ST} , ~ 0.17 eV) and ultrafast ISC ($\sim 10^9$ s⁻¹) facilitated by the heavy atom effect of the Br group (ESI[†] for details). **BBCz-SB-Br** is also advantageous because it can suppress the reabsorption of UC emission in the range of 350–420 nm (Fig. 2) and reduce energetic losses associated with ISC due to its small ΔE_{ST} .^{48–51} As UC emitters (also referred to as annihilators) functioning in the UV region, we developed **SiDPN-1** and **SiDPN-2** based on 1,4-diphenylnaphthalene (DPN). The

^a Department of Applied Chemistry, Graduate School of Engineering, Kyushu University, 744 Motoooka, Nishi-ku, Fukuoka 819-0395, Japan. E-mail: n-kimi@mail.cstm.kyushu-u.ac.jp

^b Institute for Advanced Study, Kyushu University, 744 Motoooka, Nishi-ku, Fukuoka 819-0395, Japan. E-mail: yasuda@ifrc.kyushu-u.ac.jp

Electronic Supplementary Information (ESI) available: See DOI: 10.1039/x0xx00000x

Table 1. Photophysical Data of DPN-based Emitters

emitter	state ^a	λ_{PL}^b (nm)	Φ_{PL}^c (%)	τ^d (ns)	k_r^e (10^8 s^{-1})	k_{nr}^f (10^8 s^{-1})	E_S^g (eV)	E_T^g (eV)
DPN	Sol	378	45	1.0	4.5	5.5	3.52	2.50
	Film	374	58	1.6	3.7	2.7	3.56	2.30
SiDPN-1	Sol	386	54	1.0	5.2	4.5	3.45	2.50
	Film	390	53	1.0	5.2	4.6	3.52	2.30
SiDPN-2	Sol	386	54	1.0	5.6	4.8	3.43	2.45
	Film	394	52	1.0	4.9	4.5	3.47	2.27

^aSol = deoxygenated toluene solution with a DPN subunit concentration of 20 mM; Film = neat film of 1 μm thickness. ^bPL emission maximum. ^cAbsolute PL quantum yield evaluated using an integrating sphere under N_2 . ^dPL lifetime. ^eRate constant of fluorescence radiative decay ($S_1 \rightarrow S_0$): $k_r = \Phi_{PL}/\tau$. ^fRate constant of nonradiative decay: $k_{nr} = (1 - \Phi_{PL})/\tau$. ^gLowest excited singlet (E_S) and triplet (E_T) energies estimated from onset wavelengths of the fluorescence and low-temperature phosphorescence spectra recorded at 300 and 77 K, respectively.

basic photophysical properties of these emitters and sensitizer are presented in Fig. 2 and Table 1. Introducing a bulky tetraphenylsilane moiety allows the emitters to form thermodynamically stable glassy solids. **SiDPN-2** is anticipated to perform better than **SiDPN-1**, especially in solid-state TTA-UC, because of the relatively high density of DPN subunits and potential for inter- and intramolecular TET and TTA.^{32,52-56}

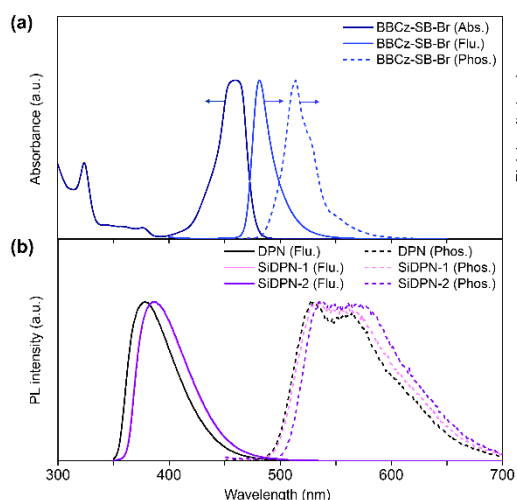


Fig 2. (a) UV-vis absorption, fluorescence (300 K), and phosphorescence (77 K) spectra of **BBCz-SB-Br** photosensitizer and (b) Fluorescence (300 K) and phosphorescence (77 K) spectra of DPN-based emitters in deaerated toluene solutions.

To verify the intrinsic potential of the three UC emitters (**DPN**, **SiDPN-1**, and **SiDPN-2**), we first investigated their TTA-UC properties in deaerated toluene solutions in combination with the **BBCz-SB-Br** photosensitizer, which possesses the S_1 and T_1 excitation energies (E_S and E_T) of 2.66 and 2.53 eV, respectively (Fig. 3). All TTA-UC measurements in solutions were performed under unified conditions with a photosensitizer concentration of 100 μM and an emitter DPN subunit concentration of 20 mM. Under excitation with a 445 nm laser, distinct UC emissions peaking at 370–390 nm in the UV region were observed for all three solution samples (Fig. 3a). As expected, the triplet-mediated UC emissions decayed in milliseconds (Fig. 3b). The TTA-UC efficiencies ($\eta_{UC} \equiv 2\Phi_{UC}$, standardized to 100% for the theoretical limit) of the **SiDPN-1** and **SiDPN-2** solutions reached 15.8% and 16.2%, respectively, which were marginally higher than that of the **DPN** solution (14.8%) measured at the same

excitation intensities (Fig. 3c). This trend is consistent with the variation in photoluminescence quantum yields (Φ_{PL}) of the emitters in solutions (Table 1). As shown in Fig. 3d, the excitation power dependence of the UC emission intensity for the three solution samples clearly demonstrated a quadratic-to-linear change in the correlation slopes; this behavior is a typical feature of TTA-UC.⁵⁷⁻⁵⁹ The threshold excitation intensities (I_{th}), defined as the intersection of these two fitting lines, were estimated to be 35, 11, and 31 mW cm^{-2} for **DPN**, **SiDPN-1**, and **SiDPN-2**, respectively, combined with **BBCz-SB-Br**.

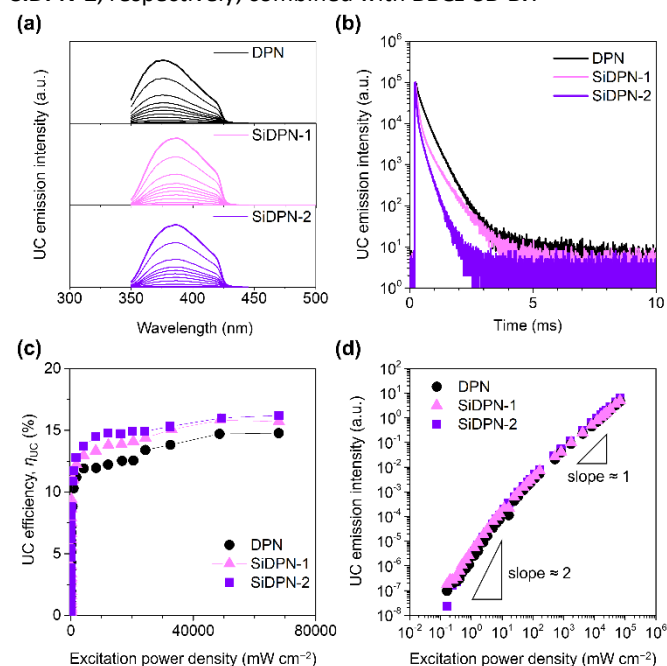


Fig 3. TTA-UC characteristics of deaerated toluene solutions containing **BBCz-SB-Br** photosensitizer and DPN-based emitters under photoexcitation at 445 nm ([**BBCz-SB-Br**] = 100 μM , [**DPN**] = 20 mM, [**SiDPN-1**] = 20 mM, and [**SiDPN-2**] = 10 mM). (a) UC emission spectra recorded at excitation power densities ranging from 0.1 mW cm^{-2} to 68 mW cm^{-2} with a 425 nm shortpass filter, (b) UC emission decay curves, (c) UC efficiency (η_{UC}) as a function of excitation power density, and (d) double logarithmic plots of UC emission intensity versus excitation power density.

To study the Dexter-type TET behavior in TTA-UC, we performed Stern–Volmer quenching experiments (ESI[†]). Increasing the concentration of the emitters in each solution led to a gradual reduction in the delayed fluorescence lifetime of

the **BBCz-SB-Br** photosensitizer. The TET quantum yields (Φ_{TET}) derived from the Stern–Volmer analysis were as high as $\geq 99\%$ for the experimental concentration conditions depicted in Fig. 3, revealing highly efficient TET processes with negligible backward energy transfer. In general, η_{UC} is described by Eq. (1), by considering the quantum efficiency of each photophysical process within the whole system:

$$\eta_{\text{UC}} = f \cdot \Phi_{\text{ISC}} \cdot \Phi_{\text{TET}} \cdot \Phi_{\text{TTA}} \cdot \Phi_{\text{PL}} \quad (1)$$

where f is the spin statistical factor (or singlet generation efficiency), Φ_{ISC} is the ISC quantum yield of the photosensitizer, and Φ_{TTA} is the TTA quantum yield. For the present TTA-UC systems under excitation intensities above I_{th} , the Φ_{ISC} , Φ_{TET} , and Φ_{TTA} values can be assumed to be close to unity; the f values are therefore estimated to be 29% and 30% for **SiDPN-1** and **SiDPN-2**, respectively (the theoretical maximum $f = 40\%$). In the solution systems, in which molecular diffusion governs the TET processes, no significant difference is observed in the overall TTA-UC behavior between these two emitters at the same DPN subunit concentration ($[\text{DPN}] = 20 \text{ mM}$).

To demonstrate all-solid-state TTA-UC, we fabricated and evaluated binary solid films with a thickness of $\sim 1 \mu\text{m}$, in which a small amount of the **BBCz-SB-Br** photosensitizer (0.1–0.2 mol%) was dispersed in a host matrix of the DPN-based emitter (Fig. 4 and ESI†). Although the **DPN**-hosted film was polycrystalline, the **SiDPN-1**- and **SiDPN-2**-hosted films were amorphous and therefore, transparent (Fig. 4a).⁶⁰ Indeed, such thicker films retained $>98\%$ transmittance over the entire visible range, except for the narrow absorption band at $\sim 460 \text{ nm}$ for the **BBCz-SB-Br** photosensitizer (ESI†). More importantly, **DPN**, **SiDPN-1**, and **SiDPN-2** retained high Φ_{PL} values (52%–58%) in the solid films, comparable to those in the foregoing solution states (Table 1). These notable features allowed the DPN derivatives to function not only as emitters but also as effective glassy matrices (without the need for an additional host) for solid-state TTA-UC.

UC emissions in the same UV region were clearly observed even in the binary solid films upon excitation at 445 nm (Fig. 4b) similar to those in the solution states. While the polycrystalline **DPN**-hosted film displayed a relatively short UC emission lifetime (τ_{UC}) of $\sim 0.1 \text{ ms}$, those for the amorphous **SiDPN-1**- and **SiDPN-2**-hosted films were significantly prolonged to 2.8 and 1.4 ms, respectively (Fig. 4c). The I_{th} for the **SiDPN-1**- and **SiDPN-2**-hosted films were as low as 49 and 44 mW cm^{-2} , respectively, and their η_{UC} values, determined by the absolute method, exceeded 2% (Fig. 4d,e). By contrast, the **DPN**-hosted film exhibited a relatively higher I_{th} of 134 mW cm^{-2} and a lower η_{UC} of 1.6%. The lower TTA-UC performance of the **DPN**-hosted film can presumably be partially attributed to agglomeration of the photosensitizer and/or inhomogeneous (discontinuous) grain formation due to emitter crystallization. Thus far, a high η_{UC} of 8.6% has been reported for solid-state visible-to-UV TTA-UC combining 3,3'-carbonylbis(7-diethylaminocoumarin) (CBDAC) as a sensitizer and 2,5-diphenyloxazole (PPO) as an emitter.⁴³ Although our present system is somewhat less efficient, it enables UC emissions in the form of transparent solid films.

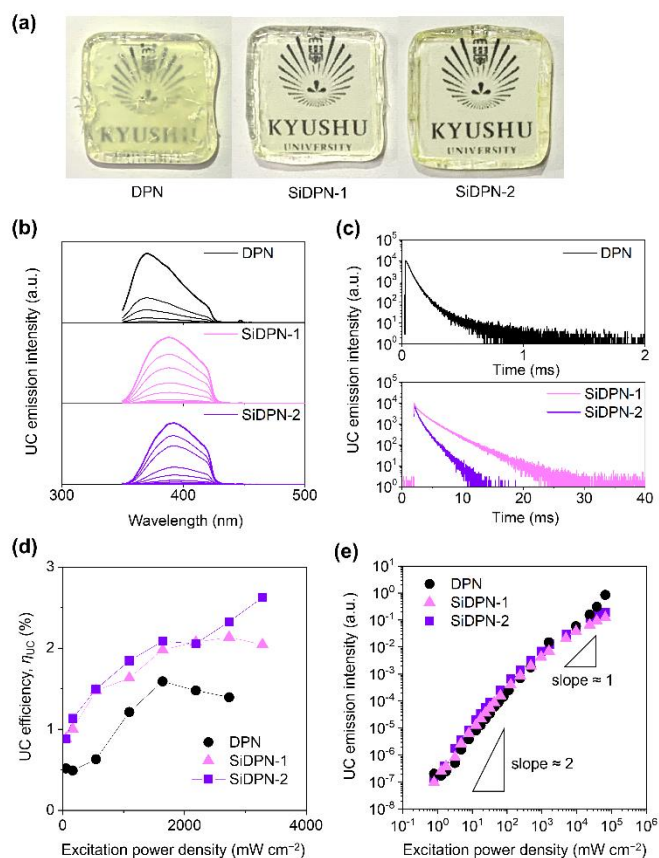


Fig. 4 All-solid-state TTA-UC characteristics. (a) Photos of $1 \mu\text{m}$ -thick **DPN**, **SiDPN-1**, and **SiDPN-2** films ($15 \text{ mm} \times 15 \text{ mm}$) containing **BBCz-SB-Br** photosensitizer ($[\text{BBCz-SB-Br}] = 0.1 \text{ mol\%}$ for **DPN** and **SiDPN-1**; 0.2 mol\% for **SiDPN-2**) taken under room light. (b) UC emission spectra under photoexcitation at 445 nm and power densities ranging from 0.8 mW cm^{-2} to 67 W cm^{-2} , (c) UC emission decay curves, (d) UC efficiency (η_{UC}) as a function of excitation power density, and (e) double logarithmic plots of UC emission intensity versus excitation power density.

To gain insight into the impact of the molecular structures of the emitter on triplet energy migration and TTA, we further estimated the triplet exciton diffusion constants (D_{T}) from the experimental I_{th} , according to Eqs. (2) and (3).⁵⁷

$$I_{\text{th}} = (\alpha \cdot \Phi_{\text{TET}} \cdot \gamma_{\text{TT}})^{-1} \cdot (\tau_{\text{T}})^{-2} \quad (2)$$

$$\gamma_{\text{TT}} = 8\pi a_0 D_{\text{T}} \quad (3)$$

where α is the absorption coefficient of the photosensitizer at the excitation wavelength ($\alpha = 780$ and 1700 cm^{-1} for the **SiDPN-1**- and **SiDPN-2**-hosted films, respectively), γ_{TT} is the second-order annihilation constant, τ_{T} is the emitter triplet lifetime ($\tau_{\text{T}} \approx 2\tau_{\text{UC}}$),⁶¹ and a_0 is the annihilation distance of triplets (assumed to be $\sim 0.9 \text{ nm}$).^{57,62} Here, $\Phi_{\text{TET}} \approx 1$ is assumed because the intermolecular distances between the photosensitizer and emitters are considered close enough to TET in these solid films. Consequently, the D_{T} value of twin **SiDPN-2** ($3.6 \times 10^{-10} \text{ cm}^2 \text{ s}^{-1}$) was twice as much that of **SiDPN-1** ($1.8 \times 10^{-10} \text{ cm}^2 \text{ s}^{-1}$). The larger D_{T} and shorter τ_{UC} of the **SiDPN-2** film than the **SiDPN-1** film can be primarily attributed to the relatively higher density of DPN subunits in the films. In the **SiDPN-2** film, another additional possibility is the contribution from intramolecular TET and TTA^{32,52–56} in addition to the common intermolecular processes; the proximity of the

two DPN units can allow for faster TTA, accelerating the UC emission decay (Fig. 4c).

In summary, using a judiciously selected combination of DPN-based glass-forming emitters and a MR-TADF-type photosensitizer, we demonstrated metal-free, solid-state visible-to-UV TTA-UC with high processability and transparency. The photophysical analyses revealed that the design strategy of twin emitters such as **SiDPN-2** is particularly useful for the development of efficient solid-state TTA-UC systems. We believe that the findings obtained in this study will contribute to further improving the efficiency of solid-state visible-to-UV TTA-UC and developing their practical applications.

This work was supported in part by Grant-in-Aid for JSPS KAKENHI (Grant No. JP21H04694 and JP20H05676) and JST CREST (Grant No. JPMJCR2105). The authors are grateful for the support provided by the Cooperative Research Program of "Network Joint Center for Materials and Devices".

Author Contributions

T.Y. conceptualized the project; S.W. synthesized the materials; S.W. and K.M. performed spectroscopic measurements and analysis; S.W. and T.Y. wrote the manuscript; N.K. and T.Y. supervised the entire research project.

Conflicts of interest

There are no conflicts to declare.

References and notes

- J. Zhou, Q. Liu, W. Feng, Y. Sun and F. Li, *Chem. Rev.*, 2015, **115**, 395–465.
- S. Balushev, T. Miteva, V. Yakutkin, G. Nelles, A. Yasuda and G. Wegner, *Phys. Rev. Lett.*, 2006, **97**, 143903.
- T. N. Singh-Rachford and F. N. Castellano, *Coord. Chem. Rev.*, 2010, **254**, 2560–2573.
- J. Zhao and S. Ji and H. Guo, *RSC Adv.*, 2011, **1**, 937–950.
- A. Monguzzi, R. Tubino, S. Hoseinkhani, M. Campione and F. Meinardi, *Phys. Chem. Chem. Phys.*, 2012, **14**, 4322–4332.
- Y. C. Simon and C. Weder, *J. Mater. Chem.*, 2012, **22**, 20817–20830.
- V. Gray, D. Dzebo, M. Abrahamsson, B. Albinsson and K. Moth-Poulsen, *Phys. Chem. Chem. Phys.*, 2014, **16**, 10345–10352.
- T. W. Schmidt and F. N. Castellano, *J. Phys. Chem. Lett.*, 2014, **5**, 4062–4072.
- T. F. Schulze and T. W. Schmidt, *Energy Environ. Sci.*, 2015, **8**, 103–125.
- N. Yanai and N. Kimizuka, *Acc. Chem. Res.*, 2017, **50**, 2487–2495.
- P. Bharmoria, H. Bildirir and K. Moth-Poulsen, *Chem. Soc. Rev.*, 2020, **49**, 6529–6554.
- C. Gao, W. W. H. Wong, Z. Qin, S.-C. Lo, E. B. Namdas, H. Dong and W. Hu, *Adv. Mater.*, 2021, **33**, 2100704.
- L. Zeng, L. Huang, J. Han and G. Han, *Acc. Chem. Res.*, 2022, **55**, 2604–0615.
- M. Uji, T. J. B. Zähringer, C. Kerzig and N. Yanai, *Angew. Chem. Int. Ed.*, 2023, **62**, e202301506.
- B. S. Richards, D. Hudry, D. Busko, A. Turshatov and I. A. Howard, *Chem. Rev.*, 2021, **121**, 9165–9195.
- J.-H. Kim and J.-H. Kim, *J. Am. Chem. Soc.*, 2012, **134**, 17478–17481.
- M. Majek, U. Faltermeier, B. Dick, R. Pérez-Ruiz and A. Jacobi von Wangelin, *Chem. Eur. J.*, 2015, **21**, 15496–15501.
- M. Barawi, F. Fresno, R. Pérez-Ruiz and V. A. de la Pena O'Shea, *ACS Appl. Energy Mater.*, 2019, **2**, 207–211.
- B. D. Ravetz, A. B. Pun, E. M. Churchill, D. N. Congreve, T. Rovis and L. M. Campos, *Nature*, 2019, **565**, 343–346.
- B. Pfund, D. M. Steffen, M. R. Schreier, M.-S. Bertrams, C. Ye, K. Börjesson, O. S. Wenger and C. Kerzig, *J. Am. Chem. Soc.*, 2020, **142**, 10468–10476.
- M. J. Bennison, A. R. Collins, B. Zhang and R. C. Evans, *Macromolecules*, 2021, **54**, 5287–5303.
- P. B. Merkel and J. P. Dinnocenzo, *J. Lumin.*, 2009, **129**, 303–306.
- A. J. Svagan, D. Busko, Y. Avlasevich, G. Glasser, S. Balushev and K. Landfester, *ACS Nano*, 2014, **8**, 8198–8207.
- A. Monguzzi, M. Mauri, A. Bianchi, M. K. Dibbanti, R. Simonutti and F. Meinardi, *J. Phys. Chem. C*, 2016, **120**, 2609–2614.
- J. Peng, X. Guo, X. Jiang, D. Zhao and Y. Ma, *Chem. Sci.*, 2016, **7**, 1233–1237.
- X. Jiang, X. Guo, J. Peng, D. Zhao and Y. Ma, *ACS Appl. Mater. Interfaces*, 2016, **8**, 11441–11449.
- R. Vadrucci, A. Monguzzi, F. Saenz, B. D. Wilts, Y. C. Simon and C. Weder, *Adv. Mater.*, 2017, **29**, 1702992.
- A. Turshatov, D. Busko, N. Kiseleva, S. L. Grage, I. A. Howard and B. S. Richard, *ACS Appl. Mater. Interfaces*, 2017, **9**, 8280–8286.
- C. Gao, B. Zhang, C. R. Hall, L. Li, Y. Chen, Y. Zeng, T. A. Smith and W. W. H. Wong, *Phys. Chem. Chem. Phys.*, 2020, **22**, 6300–6307.
- F. Saenz, A. Ronchi, M. Mauri, R. Vadrucci, F. Meinardi, A. Monguzzi and C. Weder, *Adv. Funct. Mater.*, 2021, **31**, 2004495.
- P. Bharmoria, S. Hisamitsu, Y. Sasaki, T. S. Kang, M. Morikawa, B. Joarder, K. Moth-Poulsen, H. Bildirir, A. Mårtensson, N. Yanai and N. Kimizuka, *J. Mater. Chem. C*, 2021, **9**, 11655–11661.
- F. Edhborg, H. Bildirir, P. Bharmoria, K. Moth-Poulsen and B. Albinsson, *J. Phys. Chem. B*, 2021, **125**, 6255–6263.
- T. Mori, S. Hamzawy, P. Wagner, A. J. Mozer and A. Nattestad, *J. Phys. Chem. C*, 2021, **125**, 14538–14548.
- G. Luo, Y. Chen, Y. Zeng, T. Yu, J. Chen, R. Hu, G. Yang and Y. Li, *J. Phys. Chem. Lett.*, 2021, **12**, 9525–9530.
- T. Kashino, R. Haruki, M. Uji, N. Harada, M. Hosoyamada, N. Yanai and N. Kimizuka, *ACS Appl. Mater. Interfaces*, 2022, **14**, 22771–22780.
- N. Harada, M. Uji, B. Singh, N. Kimizuka and N. Yanai, *J. Mater. Chem. C*, 2023, **11**, 8002–8006.
- R. Vadrucci, C. Weder and Y. C. Simon, *Mater. Horiz.*, 2015, **2**, 120–124.
- P. Duan, N. Yanai, H. Nagatomi and N. Kimizuka, *J. Am. Chem. Soc.*, 2015, **137**, 1887–1894.
- C. Ye, J. Ma, S. Chen, J. Ge, W. Yang, Q. Zheng, X. Wang, Z. Liang and Y. Zhou, *J. Phys. Chem. C*, 2017, **121**, 20158–20164.
- M. Wu, D. N. Congreve, M. W. Wilson, J. Jean, N. Geva, M. Welborn, T. Van Voorhis, V. Bulović, M. G. Bawendi and M. A. Baldo, *Nat. Photonics*, 2016, **10**, 31–34.
- R. Vadrucci, C. Weder and Y. C. Simon, *J. Mater. Chem. C*, 2014, **2**, 2837–2841.
- S. Raišys, O. Adomėnienė, P. Adomėnas, A. Rudnick, A. Köhler and K. Kazlauskas, *J. Phys. Chem. C*, 2021, **125**, 3764–3775.
- R. Enomoto and Y. Murakami, *J. Mater. Chem. C*, 2023, **11**, 1678–1683.
- M. Yang, R. K. Konidena, S. Shikita and T. Yasuda, *J. Mater. Chem. C*, 2023, **11**, 917–922.
- T. Hatakeyama, K. Shiren, K. Nakajima, S. Nomura, S. Nakatsuka, K. Kinoshita, J. Ni, Y. Ono and T. Ikuta, *Adv. Mater.*, 2016, **28**, 2777–2781.

- 46 M. Yang, I. S. Park and T. Yasuda, *J. Am. Chem. Soc.*, 2020, **142**, 19468–19472.
- 47 H. J. Kim and T. Yasuda, *Adv. Optical Mater.*, 2022, **10**, 2201714.
- 48 Y. Wei, K. Pan, X. Cao, Y. Li, X. Zhou and C. Yang, *CCS Chem.*, 2022, **4**, 3852–3863.
- 49 X. Cao, K. Pan, J. Miao, X. Lv, Z. Huang, F. Ni, X. Yin, Y. Wei and C. Yang, *J. Am. Chem. Soc.*, 2022, **144**, 22976–22984.
- 50 J.-K. Li, M.-Y. Zhang, L. Zeng, L. Huang and X.-Y. Wang, *Angew. Chem. Int. Ed.*, 2023, **62**, e202303093.
- 51 Y. Shi, H. Gou, H. Wu, S. Wan, K. Wang, J. Yu, X. Zhang and C. Ye, *J. Phys. Chem. Lett.*, 2024, **15**, 4647–4654.
- 52 D. Dzebo, K. Börjesson, V. Gry, K. Moth-Poulsen and B. Albinsson, *J. Phys. Chem. C*, 2016, **120**, 23397–23406.
- 53 C. Gao, S. K. K. Prasad, B. Zhang, M. Dvořák, M. J. Y. Tayebjee, D. R. McCamey, T. W. Schmidt, T. A. Smith and W. W. H. Wong, *J. Phys. Chem. C*, 2019, **123**, 20181–20187.
- 54 C. J. Imperiale, P. B. Green, E. G. Miller, N. H. Damrauer and M. W. B. Wilson, *J. Phys. Chem. Lett.*, 2019, **10**, 7463–7469.
- 55 W. Sun, A. Ronchi, T. Zhao, J. Han, A. Monguzzi and P. Duan, *J. Mater. Chem. C*, 2021, **9**, 14201–14208.
- 56 S. Mattiello, S. Mecca, A. Ronchi, A. Calascibetta, G. Mattioli, F. Pallini, F. Meinardi, L. Beverina and A. Monguzzi, *ACS Energy Lett.* 2022, **7**, 2435–2442.
- 57 A. Monguzzi, J. Mezyk, F. Scotognella, R. Tubino and F. Meinardi, *Phys. Rev. B Condens. Matter Mater. Phys.*, 2008, **78**, 195112.
- 58 Y. Y. Cheng, T. Khoury, R. G. C. R. Clady, M. J. Y. Tayebjee, N. J. Ekins-Daukes, M. J. Crossley and T. W. Schmidt, *Phys. Chem. Chem. Phys.*, 2010, **12**, 66–71.
- 59 A. Haefele, J. Blumhoff, R. S. Khayzer and F. N. Castellano, *J. Phys. Chem. Lett.*, 2012, **3**, 299–303.
- 60 The glass-transition temperatures (T_g) of **SiDPN-1** and **SiDPN-2** were determined to be 80 and 117 °C, respectively, from differential scanning calorimetry analysis (ESI[†]).
- 61 M. Pope, C. E. Swenberg, *Electronic Processes in Organic Crystals and Polymers*, Oxford University Press, New York, 1999.
- 62 S. Hisamitsu, N. Yanai and N. Kimizuka, *Angew. Chem. Int. Ed.*, 2015, **54**, 11550–11554.

The data supporting this article have been included as part of the Supplementary Information.